



GEOSCIENCES

Lipid biomarker profile of the Permian organic-rich shales (Irati Formation) in the northernmost of Parana Basin, Brazil

LORENA TUANE G. DE ALMEIDA, AILTON S. BRITO, GIOVANI M. CIOCCARI, ALEXANDRE A. DE SOUZA, ANA MARIA P. MIZUSAKI & SIDNEY G. DE LIMA

Abstract: The Irati Formation (Paraná Basin) is a mixed carbonate and organic-rich shale sequence intruded by Jurassic-Cretaceous basic rocks, featuring Brazil's most important oil shale deposits with different maturity levels. For the first time, the distribution of oil shale biomarkers from an outcrop section (quarry) of the Irati Formation in the northernmost Paraná Basin was analyzed by GC-MS and GC-MS/MS to determine the thermal evolution, organic matter origin and the depositional paleoenvironment. The organic-rich shale at the northernmost border of the basin has high similarity with the central and southernmost areas, indicating a primary control able to induce cyclic sedimentation in a broad (10^6 km²) and restricted environment. PCA and HCA analysis of bulk and molecular parameters showed changes in the organic matter composition and paleoenvironmental conditions throughout the stratigraphic column. Nonetheless, there are significant differences compared to the central-eastern and southern areas of the basin. Contrasting with the southern region, the north, predominates biphytane, low and medium gammacerane index. $Pr/n-C_{17}$, $Ph/n-C_{18}$, HI and OI values suggest type II/III kerogen from marine organic matter with freshwater input. Among the steranes, those of stereochemistry $\alpha\alpha$ 20R predominate over $\alpha\alpha$ 20S, and the presence of β Tm indicates the shales are less thermally evolved.

Key words: Biomarkers, black shales, Irati Formation, multivariate statistical analysis.

INTRODUCTION

The marine organic-rich shales from the lower Permian Irati Formation have a wide distribution overall Paraná Basin, reaching 10^6 km², corresponding to one of the geological formations most studied among the Brazilian sedimentary formations mainly for its unique fossiliferous occurrences. Barbosa & Gomes (1958) were the first to define the Irati deposits in the lower Taquaral Member composed of dark grey siliciclastic mudstones and siltstones with low organic carbon contents, and upper Assistencia Member, which consists of black

shale rich in immature organic matter cyclic interbedded with carbonates (Brito et al. 2024).

At the beginning of the 20th century, there has been an economic interest in the Irati Formation due to the higher Total Organic Carbon (TOC) and potential for oil shale. Since the 1980's the organic-rich shales from the Irati Formation have been industrially exploited by Petrobras (Brazil's national oil company), which led to a large number of publications, most of which are related to the characterization of the organic matter in terms of quantity, quality and thermal evolution of the central (PS sector) and southeast (RGS sector) portions of the Paraná Basin (Correa da Silva & Cornford 1985, Afonso et

al. 1991, 1994, Santos et al. 2006, Souza et al. 2008, Franco et al. 2010, Alferes et al. 2011, Goldberg & Humayun 2016, Ribas et al. 2017, Matos et al. 2017, Holanda et al. 2018, 2019, Osorio et al. 2018, Reis et al. 2018, Xavier et al. 2018, Ng et al. 2019, Almeida et al. 2020, Martins et al. 2020a, b, Rocha et al. 2020, Teixeira et al. 2020, Brito et al. 2024). Those previous studies of Irati shale show a high proportion of isoparaffins over *n*-alkanes, a high concentration of pristane and phytane isoprenoids, a low abundance of terpanes and steranes, and variable gammacerane index, which indicates that the oil comes from transitional organic matter deposited in an anoxic evaporitic marine environment. Despite the widespread occurrence of those organic-rich shales, little is known about the organic matter behavior in the rest of the Paraná Basin, like the northern border (GS sector) where the carbonate-siliciclastic content ratio is higher. Even with the predominance of carbonate, the black shale beds are sedimentologically similar to those of the PS and RGS sectors of the Paraná Basin. It is possible carbonate factory influenced the preserved amount of organic matter?

In addition, the occurrence of a considerable amount of igneous intrusion within the mixed deposits in the north portion of the Paraná Basin, well-exposed in quarries, has motivated many works about its influence over the thermal maturation of the Irati Formation as a source rock (Souza et al. 2008, Franco et al. 2010, Alferes et al. 2011, Reis et al. 2018).

Anjos & Guimarães (2008) noted that the thermal effect of the intrusive rocks modified the preexisting mineralogy of the SUCAL quarry shales (Irati Formation), forming talc and calcite, through a dolomite reaction with quartz in the anchimetamorphism zone. Souza et al. (2008) carried out a geochemical study in sections of the Irati Formation affected by igneous intrusion revealing adequate quality and quantity of

organic matter for petroleum generation in the northern region. The high values of the Spore Color Index (ICE), ranging from 4 to 10, were related to the proximity of the intrusive rock that thermally affected 6.85 m of the analyzed section. The range that shows maturation compatible with the wet/dry gas generation window is 1.8 m, while the range compatible with the oil generation window has a thickness of 5.5 m. More recently, Cioccarri & Mizusaki (2019) studied the generation aureole created by evaluation of the thermal effect of the diabase sill in the embedding rock. The result showed an increase in thermal maturation in a zone around the diabase intrusion. The stages of thermal maturation demonstrated that the supermature zone varied from the point of contact with the sill to approximately 7.4 m and the oil generation window from 7.4 to 1.2 m.

The interest in characterizing the organic matter in this unit is due to its high potential for oil generation, and the unique presence of variable levels of maturation due to igneous rocks that operate as heat sources for hydrocarbon generation. Despite many studies on the Irati Formation in Brazil's southern and southeastern regions, there is still a significant gap regarding the geological processes on the northern border of the basin, especially regarding molecular parameters (biomarker data). Toward the north of the basin predominates the shallowest conditions and thicker carbonates beds. Nevertheless, the shales also present a high potential for hydrocarbon generation. Therefore, this work presents a detailed analysis of biomarkers using GC-MS and GC-MS/MS associated with TOC and Rock-Eval data for the black shales interbedded with carbonate deposits from the Irati Formation of Paraná Basin, Brazil.

GEOLOGICAL SETTING

The intracratonic Paraná Basin is located in the central-eastern part of the South American continent, covering about 1,700,000 km² with a sedimentary column of 7,000 meters. The Irati deposits are placed at the beginning of the regressive phase of the Carboniferous-Triassic sequence (Milani et al. 2007, Holz et al. 2010). Santos et al. (2006) found a lower Permian age of 278 ± 2.2 Ma (Cisuralian) for Irati Formation using zircons from the bentic deposits within the Irati Formation. The succession is interpreted as formed in a marine paleoenvironment, characterized by shallow and relatively calm waters, with restricted communication with the open sea, and stratified water column (Lavina & Lopes 1986, Araújo et al. 2001, Brito et al. 2024). Eventual agitation of the marine environment was recorded by hummocky-type sedimentary structures (Xavier et al. 2018). The deposition of organic-rich shales, reaching 27% (of TOC) occurred in the southern portion of the basin, whose organic matter composition is oil-prone usually algal and lipid-rich (Brito et al. 2023).

The Irati Formation has an overall thickness between 40 and 70 meters, mainly composed of pyrobituminous shales, black shales, gray dolomites, nodular carbonates, siltstones and fine sandstones beds (Maraschin & Ramos 2015, Xavier et al. 2018, Brito et al. 2023). The dark gray mudstones and siltstones of the lower Taquaral Member were deposited under low dysoxic to suboxic conditions, below the storm wave base. The uppermost Assistência Member depositional system was dominated by high anoxic and salinity-stratified water column and it is composed of bituminous shales interbedded with carbonates (Reis et al. 2018, Xavier et al. 2018, Brito et al. 2023). Many studies on the Irati Formation is also motivated due to its fossiliferous content, composed predominantly

of aquatic reptiles and floras, correlated with the Whitehill Formation in southern Africa, which indicates that during the Permian period, both continents formed a unique continental mass denominated Supercontinent Gondwana (Barberena & Timm 2001, Guerra-Sommer & Cazzulo-Klepzig 2001, Maraschin & Ramos 2015).

MATERIALS AND METHODS

Sampling and Bulk Organic Matter Analysis

The organic-rich shales were sampled from a stratigraphic section at the SUCAL quarry, an excellent exposure of the Irati Formation located in the northern part of the Paraná Basin (GS sector - Goiás state, Brazil). The samples (see the stratigraphic log in Figure 1) were analyzed for TOC and Rock-Eval pyrolysis and biomarker. Before geochemical analyses, all samples were cleaned, dried at 70 °C and crushed into powder.

About 250 mg of the powdered samples were treated with hydrochloric acid (50%) at 60 °C to remove any possible inorganic carbon. Then, the samples were combusted in a LECO SC-444 instrument for Total Organic Carbon (TOC) contents (wt%). Pyrolysis analyses were performed using Rock-Eval 6 (VINCI Technologies) equipment, using about 80 mg of sample, heated from 300 to 650 °C with a heating rate of 25 °C/min in a helium atmosphere.

Extraction and fractioning

The samples were ground and subjected to three successive extractions with 50 mL of dichloromethane/methanol (88:12 v/v). The extraction procedure was carried out in an ultrasonic bath, approximately 500 mg of powdered copper metal was added to obtained extract for sulfur removal for 30 min at 60 °C. After filtration, the solvent was removed using a rotary evaporator.

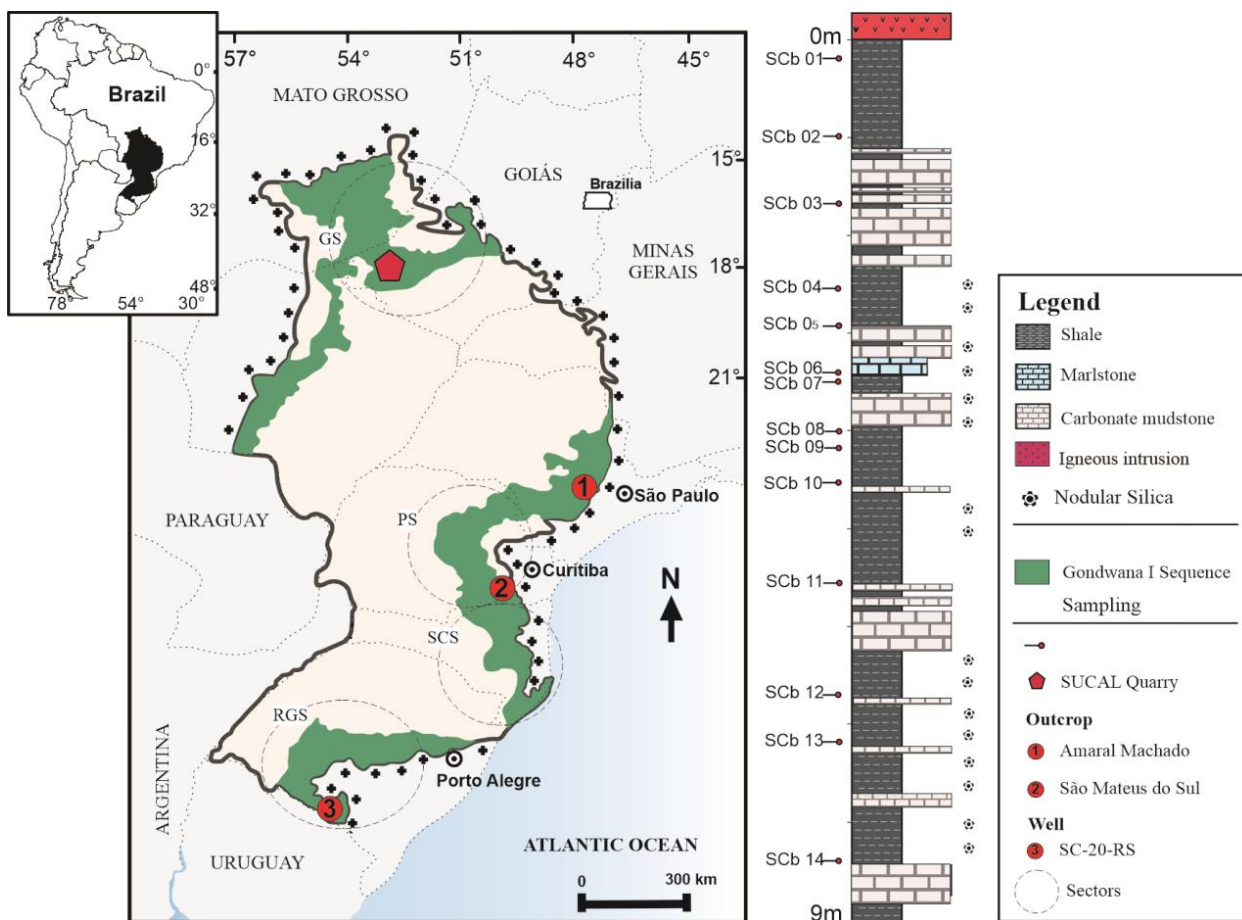


Figure 1. Geological map showing the Paraná Basin and studied samples location (northern area, GS sector). Previously studied areas of the Irati Formation which were used in the work are from (1) Amaral Machado (São Paulo state, northeastern border); (2) São Mateus do Sul (Paraná state, central east area - PS sector); (3) Rio Grande do Sul state, southern area - RGS sector).

For neutral biomarkers analysis, aliquots of 50 mg of each extract were fractionated into three fractions (aliphatic, aromatic and polar) by atmospheric pressure liquid chromatography with silica (60-230 mesh, Sigma-Aldrich) impregnated with AgNO_3 (10%) as stationary phase, according to Moura et al. 2015 methodology. The fractions were eluted using *n*-hexane (aliphatic fraction), *n*-hexane/ethyl acetate 12% (88:12 v/v, aromatic fraction) and ethyl acetate/methanol 5% (95:5 v/v, polar fraction).

Urea Adduct

The samples SCb-04, SCb-07 and SCb-11 were submitted to urea treatment and the aliphatic fractions were separated into linear and branched-cyclic fractions. Briefly, 1 mL of a urea/methanol solution ($0.3 \text{ g}\cdot\text{mL}^{-1}$) was added to the aliphatic fraction dissolved in *n*-hexane:acetone (2:1 v/v), the urea crystals were solubilized using a 50 °C water bath and then cooled at room temperature for the urea recrystallization. After that, the solution was kept at 0 °C for 12 h and the crystals were dried with a nitrogen flow.

The branched-cyclic fraction was obtained by washing the crystals with *n*-hexane 2 mL (five times) and after this, it was filtered through

anhydrous sodium sulfate, evaporated under reduced pressure and placed in a glass bottle.

The urea crystals were solubilized in distilled water for the *n*-alkanes recovery; liquid-liquid extraction was performed repeatedly with 2 mL of *n*-hexane and the organic phase was filtered through anhydrous sodium sulfate, evaporated under reduced pressure and placed in a glass bottle (Marotta et al. 2014).

Gas Chromatography-Mass Spectrometry analysis

The saturated and aromatic fractions were analyzed by a Shimadzu GCMS-QP2010 SE equipped with AOC-5000 auto-injector, according to the following analysis parameters: injector temperature 290 °C, split ratio of 1:10, the initial oven temperature of 60 °C (hold for 1 min). The first heating ramp was 6 °C min⁻¹ to 280 °C (remaining for 5 min). A second heating ramp was 1 °C min⁻¹ to 315 °C remaining for 15 min. A Rtx-5MS column (30 m × 0.25 mm, 0.10 μm internal film thickness with diphenyl 5% and diphenyldimethylpolysiloxane 95%) was used as stationary phase and helium as the carrier gas with a constant flow of 1.0 mL min⁻¹. The temperature of the interface and the ion source were 300 °C and 260 °C, respectively. The mass-analyzed quadrupole type operating by electronic impact (70 eV) was used for the fragments detection (47 to 650 Da). The biomarker identification was realized by comparing the retention times, order of elution and mass spectra in the scanning mode with data from the literature.

Gas Chromatography-Mass Spectrometry/Mass Spectrometry analysis

Gas Chromatography-Mass Spectrometry/Mass Spectrometry analysis was performed on ThermoScientific, TRACE GC Ultra gas chromatography, coupled to a TSQ Quantum

XLS mass spectrometer, Triple Quadrupole. The chromatographic separation was performed on a 30 m × 0.25 mm capillary column with a 0.10 μm inner film thickness coated with dimethylpolysiloxane 100% (EquityTM-1, PerkinElmer). The split/splitless PVT injector temperature at 290 °C was used in split mode (1:10), oven temperature of 60 °C holding for 4 min, with a first heating ramp of 6 °C min⁻¹ to 280 °C holding for 5 min and then a second heating ramp of 1 °C min⁻¹ to 310 °C remaining for 10 min. Helium (99.9999%) was used as a carrier gas with a constant flow of 1.0 mL min⁻¹. The triple quadrupole was operated in full scan mode with a mass range of 50 to 600 Da. The transfer line and ion source temperatures were 300 °C and 230 °C, respectively, operating in electron impact mode with an ionization energy of 70 eV.

The analysis conditions have been optimized, so then, precursor and productions were selected. The samples were reanalyzed according to the appropriate collision energy for the proposed fragmentations: energy collision of 70 eV, collision gas pressure (argon) was maintained at 1 mTorr, and scan cycle time was 1 s. The identification of biomarkers was performed by comparing the retention times, order of elution and mass spectra in the scanning mode with data from the literature.

Statistical analysis data was performed with the Origin Pro 2018 software to carry out the PCA (principal component analysis) and HCA (hierarchical cluster analysis) to identify the different types of kerogens and the variation of biomarker parameters along the stratigraphic profile.

RESULTS AND DISCUSSION

Quality and quantity of organic matter

TOC contents ranged from 0.59 to 3.18% (Supplementary Material - Figure S1 and Table S1). The high oscillation in the amount of TOC directly reflects the sedimentary process and fluctuation record in the carbonate-siliciclastic bedding. The highest amounts of organic matter are recorded in three intervals of the stratification section (TOC about 3.00% for SCb-04, SCb-07 and SCb-12 samples). The higher peak occurs in a very thin black shale bed interbedded with thicker carbonate beds (SCb-07 sample), which also coincides with the higher amount of S1 (free hydrocarbons), S2 (source rock potential) and HI (hydrogen index). In addition, the OI (oxygen index) is lower, reflecting a good paleoenvironment condition of the northern area of the Paraná Basin for organic matter preservation, possibly related to flooding surfaces.

The paleoenvironment depositional conditions of the northern part of the Irati Sea was very different from the central and southern portions, where there was significant deposition of organic matter. The TOC content shows values up to 27% for the shales related to the chemostratigraphic unit D (Alferes et al. 2011, Reis et al. 2018, Xavier et al. 2018, Brito et al. 2023).

Organic matter type and potential generating

The S1 and S2 pyrolysis data yields in the range of 0.03-5.49 and 0.03-12.45 mg HC/g rock, respectively. HI values ranged between 141-392 mg HC/g TOC, except SCb-01 and SCb-02, which showed low values (5 and 23 mg HC/g TOC, respectively). The S2 versus TOC ratio (Supplementary Material - Figure S2a) showed that the Irati Formation shales in the GS sector are considered poor to fair oil source rocks (TOC versus HI, Figure S2b). The stratigraphical

interval with the highest amount of organic matter (SCb-07 sample) also represents the better source rock with the highest S2 value among the samples.

S1 versus TOC (Figure S3a) can be used to distinguish between allochthonous (nonindigenous) and autochthonous (indigenous) hydrocarbons (Rabbani & Kamali 2005, Nady et al. 2015, Mashhadi & Rabbani 2015). The predominance of allochthonous hydrocarbons (Figure S3a) indicates that oil generation and primary migration occurred. According to Peters & Cassa (1993), mature oil-prone source rocks commonly show Bitumen/TOC ratios (Figure S1) in the range of 0.05-0.25. The Irati Formation samples showed high values for this ratio (0.30 to 0.62), except for SCb-01 and SCb-02 samples. Values higher than 0.25 can indicate contamination or migrated oil. Nevertheless, PI versus Tmax (Figure S3b) indicated a mature source rock. The kerogen type for most samples is type II/III (Figure S4). Toward the top of the succession (SCb-01 and SCb-02 samples) kerogen type III dominates. That could be due to their proximity to the igneous intrusion or a high input of oxidized organic matter. The heat gradually increases towards the dykes, increasing the degree of pyrolysis of the kerogen due to thermal stress, kerogen types III can thus be formed.

For PCA and HCA analyses, TOC and Rock-Eval (S1, S2, HI, OI, PI and Tmax) standardized data were used. The PCA (Figure 2a) demonstrates that the first three factors explain 89.3% (PC1 = 63.4%, PC2 = 14.7% and PC3 11.2%) of the variance. The Irati Formation samples, when analyzed by PCA and HCA (Figure 2) showed three groups related to three organic matter types.

Group 1 is formed by SCb-01 and SCb-02 samples that have shown the lowest TOC, HI, S1 and S2 parameters, related to their proximity

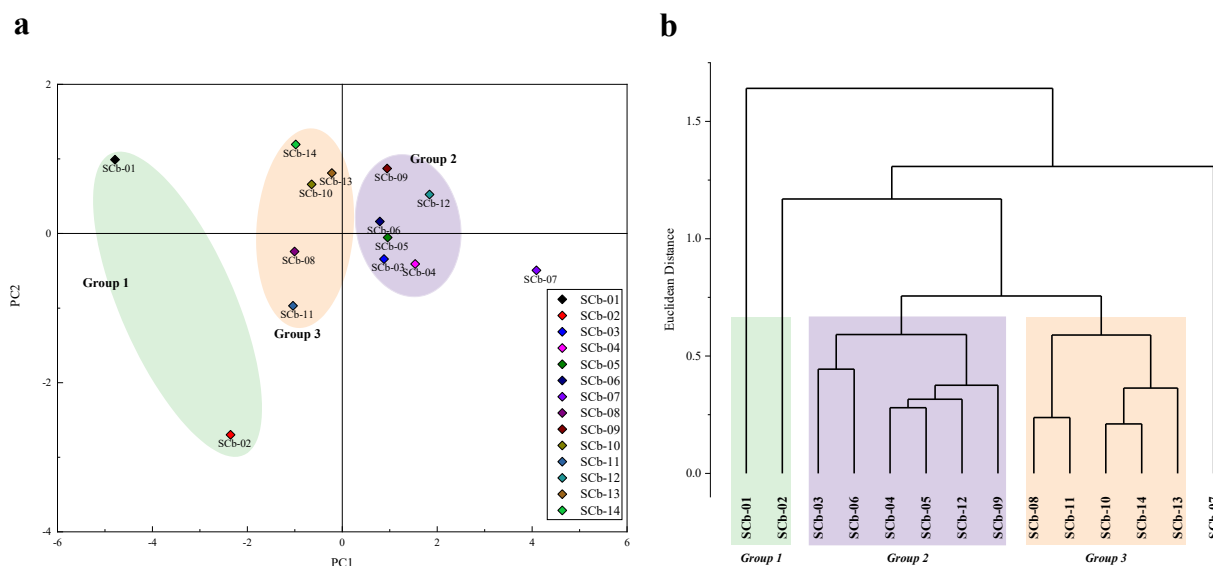


Figure 2. (a) Plot of the loadings for first and second principal components (PC1 versus PC2) and (b) Dendrogram of hierarchical cluster analysis calculated using Euclidean distance for the Irati Formation shales in the GS sector.

to the igneous intrusion (0.20 and 1.00 m, respectively).

Group 2 are source rocks characterized by TOC from 1.49 to 2.97 wt%, S1 and S2 yields in the range of 2.95 to 4.19 and 4.19 to 6.06 mg HC/g rock, respectively, and HI from 180 to 334 mg HC/g rock indicating good to excellent source rocks with type I/II kerogen. The SCb-07 sample showed the highest TOC, S1, S2 and HI values and was classified as a separate group by PCA and HCA; however, analysis using the Van Krevelen diagrams showed that this sample contains type II kerogen.

Group 3 are source rocks characterized by TOC from 0.59 to 1.85 wt%, S1 and S2 yields in the range of 0.03-2.54 and 0.03-2.99 mg HC/g rock, and HI from 5 to 213 mg HC/g rock indicating fair to good source rocks with kerogen type III/IV, the SCb-02 sample is gas-prone and the SCb-01 is inert.

Molecular parameters of thermal evolution

The maximum pyrolysis temperature (T_{max}) was between 300 and 403 °C (Figure S1 and Table S1), indicating a low maturation, only sample

SCb-01 that is in direct contact with the diabase intrusion exhibited a higher value (607 °C), which indicates high thermal maturation.

Bitumen yields for the analyzed sample are high and range from 0.24 to 1.55% (Table S1), SCb-01 and SCb-02 showed the lowest yield values, 0.02 and 0.03%, respectively. Using the Saturate, Aromatic, Resins and Asphaltenes analysis data (SARA), a ternary diagram has been proposed by Tissot & Welte (1984) to classify crude oils and bituminous extracts. The samples are primarily aromatic-asphaltic (Figure S5) with slight differences between them. SCb-01 and SCb-02 exhibit aromatic-intermediate characteristics while SCb-04 and SCb-14 are classified as paraffinic and paraffinic-naphthenic.

Carbon Preference Index (CPI) and Odd-to-Even Predominance (OEP) values range from 0.45-0.77 and 0.60-0.77 (Figure 3, Table S1), respectively, showing even over odd preference for the *n*-alkanes distribution (Figure S6). CPI or OEP values significantly above (odd preference) or below (even preference) 1.0 indicate low thermal maturity. Values of 1.0 suggest that an oil or rock extract is thermally mature (Peters

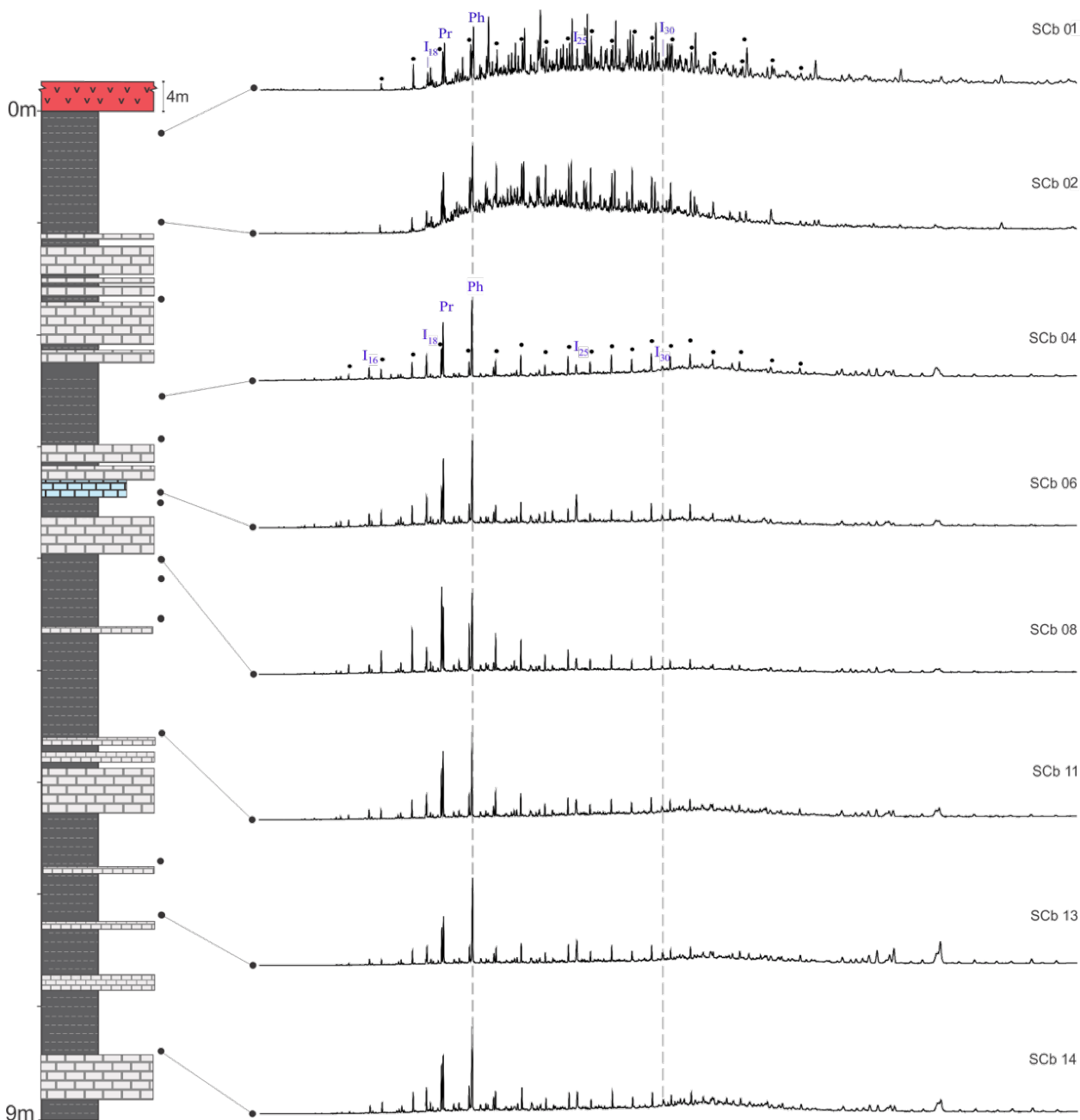


Figure 3. Total Ion Chromatogram (TIC) profile of aliphatic fractions of the Irati Formation shales in the GS sector. Pr = pristane; Ph = phytane; black dots = C₁₃ to C₃₄ n-alkanes.

et al. 2005). Just the samples closer to the diabase intrusion, SCb-01, and SCb-02 showed values ~ 1, suggesting high thermal evolution (Bray & Evans 1961, Scalan & Smith 1970, Marzi et al. 1993). The SCb-01 and SCb-02 saturated fractions chromatogram showed a large unresolved hump that indicates a complex

mixture of hydrocarbons, probably originating from thermally initiated non-selective free radical polymerization induced by the igneous intrusion.

Tricycloterpanes (TT, Figure S7) were observed in most samples, and their chromatograms varied along with the stratigraphic profile,

the samples unaffected by igneous intrusion showed TTC_{23} , TTC_{24} , and TTC_{27} . The rocks from the significantly altered zone (SCb-01 and SCb-02) present C_{19} to C_{27} homologs. Tetracyclic terpanes were observed by Grande et al. (1993) in mature oils and rock extracts from lacustrine and marine carbonate rocks, suggesting that the precursor organisms of these compounds lived in moderate salinity conditions, however, Zumberge (1983) demonstrated that thermal cleavage of the alkyl side chain into sester- and triterpenes can form C_{19} - C_{20} tricyclics.

$18\alpha(H)$ -trisneohopane (Ts) is more stable to thermal degradation than $17\alpha(H)$ -trisorhopane (Tm), so it is expected that the values of the Ts/Tm ratio will increase for oils with higher maturation. The ratio of these isomers expressed as Ts/Tm and Ts/(Ts+Tm), exhibited similar values from 0.04 to 0.41 and 0.03 to 0.39 (Figures S6 and S7, Table SI) suggesting immature samples (Seifert & Moldowan 1978, Moldowan et al. 1986, 1994, Peters et al. 2005), as observed in the Rock-Eval analysis.

The C_{27} $17\beta(H)$ -22,29,30-trisorhopane (βTm) was identified in all the samples. This compound has already been reported by Reis et al. (2018) for the PS and RGS sectors. It is characteristic of immature source rocks, as thermal maturation increases, the relative concentration of βTm is expected to decrease because it is thermally unstable when compared to Ts and Tm (Hong et al. 1986). Rock extracts from the Irati Formation showed a low relative abundance of Ts and it was practically absent at 1.68 to 8.41 m from the diabase intrusion.

Usually, the $17\beta(H)$, $21\beta(H)$ -hopanes are the dominant structures in immature sediments, although $17\beta(H)$, $21\alpha(H)$ -moretananes and $17\alpha(H)$, $21\beta(H)$ -hopanes are still present. The stability of hopanes and moretananes increases according to the sequence $\beta\beta < \beta\alpha < \alpha\beta$, with $\alpha\beta$ being the most stable. The C_{30} $\beta\alpha/(\alpha\beta+\beta\alpha)$ ratio

reached values from 0.9 to 1.0 at the beginning of the oil production, this ratio values ranged from 0.10-0.29, while the C_{31} $\alpha\beta$ $22S/(22S+22R)$ and C_{35} $\alpha\beta$ $22S/(22S+22R)$ ratios ranged from 0.26-0.55 and 0.30-0.55, respectively (Ensminger et al. 1977, Seifert & Moldowan 1980, Peters et al. 2005).

Correlation graphs for C_{29} $20S/(20S+20R)$ versus C_{29} $\alpha\beta\beta/(\alpha\beta\beta+\alpha\alpha\alpha)$ steranes and of C_{31} $22S/(22S+22R)$ homohopanes (Figures S8 and S9) are presented (Seifert & Moldowan 1978, 1980). The C_{29} $\alpha\beta\beta S/(\alpha\beta\beta+\alpha\alpha\alpha)$ ratio ranged from 0.23 to 0.31 (Table SI), which indicates an immature stage since this ratio did not reach the maximum value at 75% of conversion (Mackenzie & McKenzie 1983, Beaumont et al. 1985, Peters et al. 2005). The C_{27} and C_{29} $20S/(20S+20R)$ ratios for steranes ranged from 0.14 to 0.3, and 0.11 to 0.36, respectively, supporting the C_{29} $\alpha\beta\beta S/(\alpha\beta\beta+\alpha\alpha\alpha)$ interpretation, since this ratio reaches equilibrium value close of 0.52-0.55 (Seifert & Moldowan 1978).

In these samples, a diasterene series (Figure S10a) was identified by the m/z 257 fragments, though hop-17(21)-enes (m/z 367) were not identified. The diasterane formation involves the migration of C-10 and C-13 methyl groups to C-5 and C-14 and this process is favored by clay catalysis, acidic conditions, and/or high temperatures (Peters et al. 2005). The high abundance of diasteranes is usually associated with a low degree of thermal evolution since they are formed during diagenesis and have also been associated with immature rocks (Brassel et al. 1986).

The monoaromatic and demethylated triaromatic steranes (MA and TA) distributions (Figures S10a and S10c) are similar to that reported by Osorio et al. (2018) for Irati Formation. However, methylated triaromatic steranes (m/z 245) appear to be in low intensity or absent in the GS sector of the Irati Formation. MA(I)/MA

(I+II) and TA(I)/TA(I+II) ratios (Table S1) presented values of 0.08- 0.20 and 0.09-0.64, respectively, which is below the equilibrium value of 1.0. The samples closest to the igneous intrusion (SCb-01 and SCb-02) showed highly altered chromatographic profiles for monoaromatic and demethylated triaromatic steranes, preventing the MA (I)/MA (I+II) and TA(I)/TA(I+II) ratios calculation.

The distribution of the phenanthrene and alkyl phenanthrenes (m/z 178+192+206) of the SCb-07 sample is shown in Figure S11. In the samples with low thermal evolution the 1-MP and 9-MP (α -isomers) display a higher abundance, whereas as maturation increases, geological isomers increase (2-MP and 3-MP, β -isomers), due to the greater stability of the β positions to α positions (Peters et al. 2005, Heckmann et al. 2011). For the studied samples, the predominance of the more stable isomers (2-MP and 3-MP) over the less stable (1-MP and 9-MP) suggests medium to high maturation. The phenanthrene distribution seems to be very sensitive to the heat of the igneous intrusion. these parameters exhibited a progressive decreasing order of maturation according to the distance from the diabase intrusion.

It is well-known in the literature that igneous intrusion can act as a heat source and generate an atypical petroleum system, and so affecting the carbon skeleton of the hydrocarbons. As observed in the samples SCb-01 and SCb-02, the heat from the intrusion affected the preserved organic matter and led to a miss interpretation of the source. Analysis of data through the Van Krevelen diagram shows kerogen type III for the SCb-02, but biomarkers revealed a bacteria origin. Nevertheless, Rock-eval pyrolysis and classical biomarkers have limitations regarding the record of the igneous intrusion heat effect. Less than two meters below the igneous intrusion sill the samples have no record of its influence

(they are immature). Though, the phenanthrene and alkyl-phenanthrenes parameters showed high sensitivity to those igneous intrusion heat, and they recorded a progressive degree of its influence, becoming an excellent parameter for assessment of lateral variation degree of maturation.

Molecular parameters of organic matter source and depositional environment

The n -alkanes series ranged from C_{13} to C_{34} with a predominance of C_{15} - C_{17} , TAR<1 (Figure S12, (Table S1), and showed slightly unimodal distribution for all samples, indicating organic matter of marine origin with land plant input (Bray & Evans 1961, Scalan & Smith 1970, Mello et al. 1995).

Two distinct chromatogram types were produced for the stratigraphic profile analyzed (Figure 3). The first one is formed by the samples SCb-03 to SCb-14, which presents a low relative abundance of n -alkanes and cycloalkanes and a high relative abundance of isoprenoids (Figure S13). The second is composed of SCb-01 and SCb-02, which are closer to the diabase (0.20 and 1.00 m, respectively). They present the predominance of isoprenoids and cycloalkanes (n -alkyl cyclohexanes, methyl n -alkylcyclopentanes, macrocyclic alkanes, and 1-methyl-macrocyclic alkanes).

n -Alkyl cyclohexanes and related compounds, such as alkyl phenols, are important compounds among the set of sedimentary hydrocarbons. Cyclohexyl fatty acids are potential precursors that are found in some thermophilic and non-thermophilic bacteria. However, limited distributions of the amount of carbon in biological lipids are observed when compared to the long-length carbon chain found in sediments, suggesting less exotic sources for these compounds (Brocks & Summons 2014). Pyrolysis products of aliphatic polyaldehydes, algae, and fatty acids can represent a wide

variety of alkyl cyclohexanes (Rubinstein & Strausz 1979, Fowler et al. 1986, Gelin et al. 1994).

The relative proportion of the three groups of *n*-alkanes, $n\text{-C}_{13-18}$, $n\text{-C}_{19-24}$, and $n\text{-C}_{25-35}$ (Supplementary Material - Table SI) were calculated. These groups are related to the three main biological sources producing fatty acids: i) zooplankton and phytoplankton; ii) bacteria, and; iii) land plants (Tissot & Welte 1984, Fabiańska et al. 2013). SCb-05 to SCb-03 and SCb-01 samples have *n*-alkanes predominance in the range of $n\text{-C}_{25-33}$. SCb-12, SCb-10, SCb-09, SCb-07 and SCb-02 show the highest abundance of $n\text{-C}_{19-24}$ compounds while SCb-14, SCb-13, SCb-11, SCb-08 and SCb-06 have a higher content of *n*-alkanes in the first group ($n\text{-C}_{13-18}$).

The treatment of the samples with urea allowed the identification of isoprenoids I_{18} , I_{21} , I_{25} , I_{30} , I_{39} and I_{40} (biphytane) (Figure S14). The low relative abundance of linear *n*-alkanes and the predominance of isoprenoids and branched alkanes are also typical of organic matter from an aquatic origin in environments with high salinity (Alferes et al. 2011). A significant source of biphytane is caldarchaeol, a lipid found in the cell membrane of methanogens and members of the kingdom Crenarchaeota (Kates 1993, Koga et al. 1993). Crenarchaeote and some methanogenic organisms are capable of producing polar lipids with caldarchaeol core variants and occasionally with cyclohexane and cyclopentane rings.

In general, the Irati Formation located in the central-eastern (PS and GRS sectors) of Paraná Basin was deposited in a deeper marine setting with lower salinity when compared to the northeastern basin. The depositional system in this region exhibits a shallower marine environment with reducing bottom water conditions (Martins et al. 2020c). Martins et al. (2020b) identified β -carotane in Irati Formation samples from the northeastern and central-eastern Paraná Basin (southern Brazil).

β -Carotane can be produced by halophilic bacteria, this compound is usually found in some crude oils from source rocks formed in arid and lacustrine settings, but it's rare or low in oils from marine sources (Jiang & Fowler 1986, Clark & Philp 1989), therefore, the presence of β -carotane was associated with freshwater influxes.

Pristane (Pr) and Phytane (Ph) were the main isoprenoids detected in the Irati Formation. In the GS sector, the Pr/Ph ratio showed values between 0.44-0.76 (Figure S12), indicating an anoxic depositional environment. This parameter is generally used for the evaluation of the depositional environment redox conditions and despite the limitations of this approach, it can be quickly and easily measured. Pr/Ph ratio values above 1.0 indicate the oxic depositional environment, while values <1.0 are characteristics of anoxic conditions (Didyk et al. 1978, Kelly et al. 2011, Tao et al. 2015).

The relationship between the isoprenoids Pr/ $n\text{-C}_{17}$ and Ph/ $n\text{-C}_{18}$ (Figure S15) indicates a marine setting and an anoxic depositional condition. The organic matter deposited in carbonate, marl, or marine shale systems C_{31} 22R HH/ C_{30} Hop parameter, usually has values greater than 0.25. The correlation of the DBT/P parameter (dibenzothiophene to phenanthrene ratio) to the Pr/Ph ratio (Figure S16a), in addition to the C_{31} 22R HH/ C_{30} Hop parameter versus Pr/Ph ratio, corroborates a carbonates marine system (Hughes et al. 1995). However, the four samples (SCb-11, SCb-06, SCb-02 and SCb-01) show lacustrine sulfate-poor due to very low values for Pr/Ph and DBT/P ratios. Lacustrine-like conditions have been identified for the Irati Formation and are attributed to freshwater input, which induced water column stratification (Martins et al. 2020c, Brito et al. 2023). This data demonstrates that freshwater discharges have influenced the Irati depositional system.

Tetracyclic terpanes have already been found in rock samples and oils in several depositional environments. They represent a narrow homologous series in the range C_{24} - C_{27} . However, the origin of the C_{24} tetracyclic terpane is uncertain, it is usually associated with thermal and microbial degradation of the hopanes (Tao et al. 2015). Only one homolog series was observed for the class of tetracyclic terpanes, Tet- C_{24} , since these compounds are more stable than their tricyclic analogs, and their presence may be related to hypersaline evaporitic carbonate depositional environment (Connan et al. 1986). In addition, gammacerane is a pentacyclic terpane found in large quantities in organic extracts and oils associated with saline environments (Sinninghe-Damsté et al. 1995). However, some evidence indicates that this compound comes from certain protozoa, bacteria, and other organisms (Peters et al. 2005). Its origin is still uncertain but can be formed by reducing tetrahymanol (gamacer- 3β -ol), a lipid that replaces steroids in the membrane of certain protozoa. The primary source of tetrahymanol is ciliates protozoa, which occur at the interface between oxic and anoxic zones in stratified water columns (Sinninghe-Damsté et al. 1995). The ratio between gammacerane and C_{30} - $17\alpha(H)$, $21\beta(H)$ -hopane (*iG*) showed a range from 24.23 to 105.52, indicating a high variation of salinity throughout the stratigraphic succession.

The presence of $5\alpha(H)$, $14\alpha(H)$, $17\alpha(H)$ -pregnane ($21\alpha\alpha\alpha$) and $5\alpha(H)$, $14\alpha(H)$, $17\alpha(H)$ -22-homopregnane ($22\alpha\alpha\alpha$) were observed. The occurrence of these compounds in oils and sediments has been attributed to the breaking of the lateral chain of larger molecular weight steranes. However, other authors suggest that these compounds have an unknown biological origin and are related to hypersaline environments (Peters et al. 2005).

Steranes and diasteranes were present in high concentrations, and their distributions are dominated by C_{27} sterane (cholestane), and the C_{27}/C_{29} ratio varies from 0.50 to 1.59 (Figure S12). The predominance of C_{27} steranes indicates algal/planktonic organic matter, while the high abundance of C_{29} steranes is related to terrestrial plants. In the analyzed samples, the relative abundance (%) of C_{27} and C_{29} over C_{28} sterane indicates deposition in a coastal marine shelf as present in Figure 4a (Huang & Meinschein 1979). The cross plot of Pr/*n*- C_{17} and Ph/*n*- C_{18} ratios in Figure 4b also attests to a high continental to transitional setting contribution in bulk organic matter.

The rhythmic intercalation of siliciclastic and carbonate strata of the Irati Formation is interpreted as low-energy deposits in a restricted environment, classified by Brito et al. (2024) as an outer ramp and mid to upper-ramp. Currently, these deposits are distributed from the southernmost to the central region of Brazil. The northernmost deposits of the basin (GS sector) record the most proximal facies, with the prevalence of carbonate deposits. Nevertheless, the biomarker parameters show that, despite the terrestrial contribution, an anoxic and salinity-stratified water column predominates, similar to the deeper part of the basin (PS and RGS sectors).

Aromatic steranes are formed during sediment diagenesis due to high temperatures and pressures followed by oxidation and subsequent aromatization of the sterols. Monoaromatic and triaromatic steranes are used as source indicators (eukaryotic species), useful in correlation studies and evaluation of thermal stress, as well as to evaluate maturity in sediments samples (Moldowan & Fago 1986, Mackenzie & Maxwell 1981, Peters et al. 2005). The short-chain (C_{22} and C_{23}) and long-chain (C_{27} to C_{29}) monoaromatic steranes were identified through

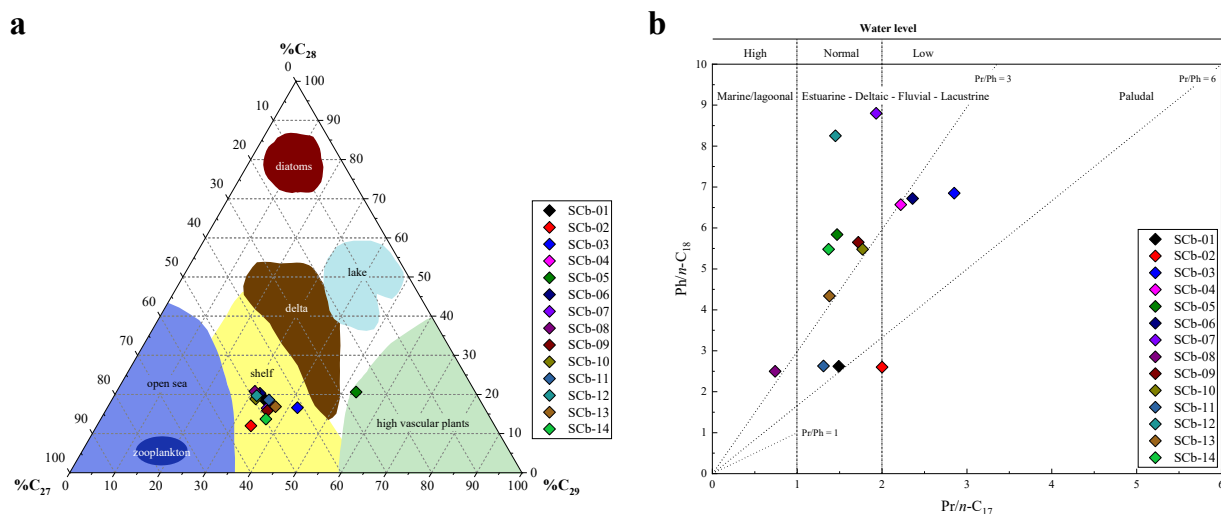


Figure 4. (a) Steranes ternary diagram (modified from Huang & Meinschein, 1979) and (b) Diagram of Pr/n-C₁₇ vs Ph/n-C₁₈ (modified from Scheffler 2004), indicating the depositional environment and primary organic matter of the Irati Formation shales in the GS sector.

the m/z 253 ions (Figure S10). Information on the depositional environment can also be provided by distributing monoaromatic steranes from the ratio between the C₂₇-C₂₈-C₂₉ carbons. In the case of the samples under study, the predominance of C₂₇ over C₂₉ monoaromatic sterane was observed, indicating low contributions of terrestrial organic matter.

PCA and HCA analysis of the biomarkers data of biological source

Standard biomarkers parameters related to the deposition paleoenvironment and organic matter source (CPI, OEP, TAR, C₁₃₋₁₈, C₁₉₋₂₄, C₁₅₋₃₃, iG , and C₂₇/C₂₉ sterane ratio) were used for PCA and HCA analysis. The Irati Formation samples, when analyzed by PCA and HCA (Figure 5b) showed three groups related to the different types of organic matter contribution.

Group-1 consists of samples SCb-01 and SCb-02, which are closer to the diabase intrusion and showed OEP and TAR ratios >1, low values iG (41.55 and 33.24%), and high relative abundance of two groups of n -alkanes, %C₁₉₋₂₄ and %C₂₅₋₃₃, which correspond to two biological sources of fatty acids, bacteria and higher vascular plants (Tissot

& Welte 1984, Fabiańska et al. 2013). Group-2 is composed of the SCb-03 and SCb-05 samples, which showed low CPI and OEP ratios (0.65-0.77 and 0.64-0.77), TAR ratio <1, medium values iG (49.58-61.95), and high relative abundance of %C₁₉₋₂₄ and %C₂₅₋₃₃ n -alkanes (33.6-35.95 and 36.18-45.93), and is related to bacteria and higher vascular plants fatty acids, as observed to the Group-1. The SCb-04 and SCb-06 to SCb-14 samples (except SCb-08) form Group 3, which exhibited low CPI and OEP ratios (0.45-0.68 and 0.60-0.75) as observed for the previous groups. However, this group shows a higher %C₁₃₋₁₈ and %C₁₉₋₂₄ n -alkanes (30.75-45.58 and 30.44-38.76), which correspond to two biological sources of fatty acids, phytoplankton/zooplankton and bacteria, low TAR and iG values (0.20-0.44 and 24.23-44.77%), just the SCb-12 showed a high iG ratio, 73.75%.

Three different groups were identified by the statistical analyses although all the samples belong to the same formation suggesting differences related to the depositional paleoenvironment and the biological organic matter source.

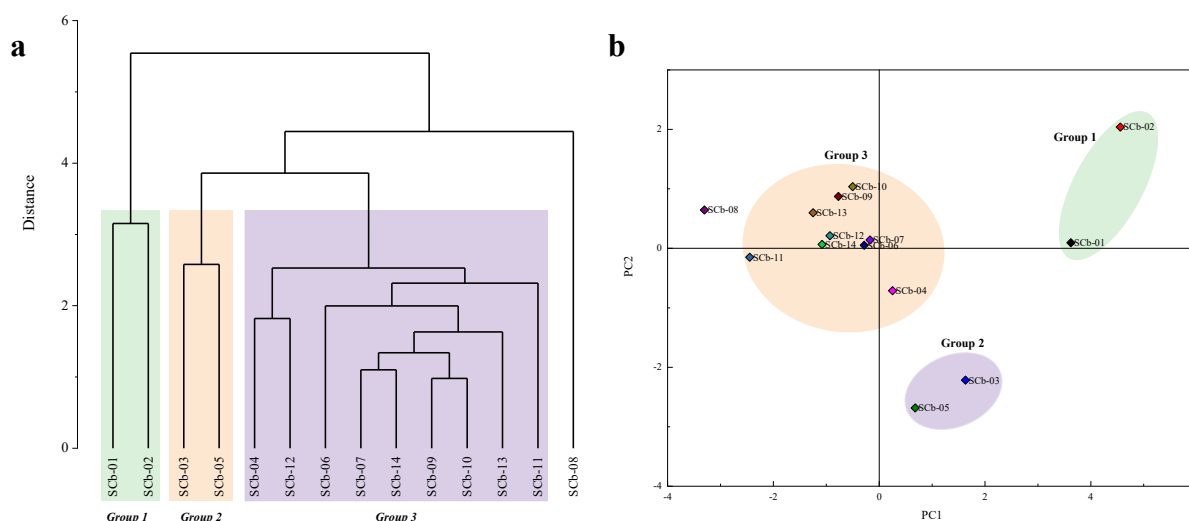


Figure 5. (a) Dendrogram of hierarchical cluster analysis calculated using Euclidean distance and (b) Plot of the loadings for first and second principal components (PC1 versus PC2) for the Irati Formation shales in the GS sector.

CPI, OEP, and C_{27}/C_{29} sterane ratios showed similar values throughout the stratigraphic succession. However, the change in the chemical composition of the three main groups of *n*-alkanes as well as the decrease in TAR and *iG* ratios with increasing depth, suggests a higher contribution of organic matter from bacteria and zooplankton/phytoplankton for base samples contrasting with the top of the stratigraphic section. The SCb-08 sample represents the peak in the GP sector of Paraná Basin with the highest *iG* and % C_{13-18} *n*-alkane group (105.52 and 53.81%) and the lowest TAR ratio, 0.11. The top samples of the stratigraphic profile showed high CPI and OEP ratios, and high relative abundance of C_{19-24} and C_{25-33} *n*-alkanes compared with the base samples. Moreover, a significant terrigenous contribution toward the top of the succession was observed by Nascimento et al. (2021) in the PS sector which was associated with a higher freshwater inflow.

CONCLUSION

The present work provided a detailed geochemical and biomarker characterization of

the northernmost shales and marlstone of the Irati Formation (GS sector). The major difference between the GS sector and the other sectors is the source rock potential for hydrocarbon generation. Pyrolysis Rock-Eval data indicate poor to moderate source rocks conditions. Only sample SCb-07 (IH=392, S2=12.45 mg HC/g rock) showed adequate quality for hydrocarbon generation. All samples had a high relative abundance of β Tm. Among the steranes, those with stereochemistry $\alpha\alpha\alpha$ 20R predominated over $\alpha\alpha\alpha$ 20S, and the presence of diasterenes suggests that the samples are less thermally evolved. The only mature or senile part of the Irati shales were those affected by igneous intrusion. Bitumen/TOC and the correlation plots of S1 versus TOC and PI versus Tmax confirm the presence of migrated hydrocarbons due to thermal stress from igneous intrusions.

Biomarker parameters and hydrocarbon distribution (the predominance of isoprenoids and the low relative abundance of linear *n*-alkanes and Pr/Ph ratio, low/medium *iG* index and the presence of Tet- C_{24}) indicate an anoxic and salinity-stratified water column prevalent in the GS sector, similarly to the PS and RGS sectors

of the basin. Freshwater input also appears to be present in the widespread Irati shales. Kerogen type II/III and freshwater discharge are corroborated by the presence of macrocyclic and 1-methyl macrocyclic alkanes, normally associated with the lacustrine alga *B. braunii*. The relative persistence of paleoenvironment conditions in the Irati Sea suggests that sedimentary mechanisms controlled the cyclic influence on the siliciclastic-limestone deposits, which the siliciclastic phase is composed of organic-rich shales. The hypersaline and highly anoxic conditions are largely due to the shallow but stagnated and restricted conditions that prevailed in the Irati Sea. The restricted depositional conditions, together with the sedimentologic and geochemical data are strong evidence for cyclic climate changes, which influenced the oscillation of deposit formation.

Acknowledgments

The authors thank PETROBRAS, Coordenação de Aperfeiçoamento de Pessoal de Nível Superior (CAPES) and Fundação de Amparo à Pesquisa do Piauí (FAPEPI) for financial support, as well as B. Timah for grammatical revision.

REFERENCES

- AFONSO JC, CARDOSO JN & SCHMAL M. 1991. Distribution and origin of organic Sulphur compounds in Irati shale oil. *Fuel* 71: 409-415.
- AFONSO JC, CARDOSO JN & SCHMAL M. 1994. Hydrocarbon distribution in the Irati shale oil. *Fuel* 73: 363-366.
- ALFERES CLF, RODRIGUES R & PEREIRA E. 2011. Geoquímica orgânica aplicada à Formação Irati, na área de São Mateus do Sul (PR), Brasil. *Geochim Bras* 27(1): 47-54.
- ALMEIDA NS, SAWAKUCHI HO, TEIXEIRA CAS, BERTASSOLI JR DJ, FURUKAWA LY, PELISSARI M & SAWAKUCHI AO. 2020. Incubation experiments to constrain the production of methane and carbon dioxide in organic-rich shales of the Permian Irati Formation, Paraná Basin. *Mar Pet Geol* 112: 104039.
- ANJOS CWD & GUIMARÃES EM. 2008. Metamorfismo de contato nas rochas da Formação Irati (Permiano), norte do Paraná. *Braz J Geol* 38(4): 629-641.
- ARAÚJO LM, RODRIGUES R & SCHERER CMS. 2001. Sequências deposicionais Irati: arcabouço quimioestratigráfico e inferências paleoambientais. *Cienc Tecn Pet* 20: 193-202.
- BARBERENA D & TIMM LL. 2001. Características estruturais dos Mesossauros e suas adaptações ao meio aquático. In: Holz M & De Ros LF. *Paleontologia do Rio Grande do Sul, Porto Alegre, CIGO/UFRGS*, p. 194-209.
- BARBOSA O & GOMES FA. 1958. Pesquisa de petróleo na Bacia do Rio Corumbataí, Estado de São Paulo. *Divisão de Geologia Mineral – DNPM, Boletim* 171: 40.
- BEAUMONT C, BOUTLIER R, MACKENZIE AS & RULLKOTTER J. 1985. Isomerization and aromatization of hydrocarbons and the paleothermometry and burial history of Alberta Foreland Basin. *AAPG Bull-Am Assoc Petr Geol* 69: 546-566.
- BRASSEL SC, EGLINTON G & MO FJ. 1986. Biological marker compounds as indicator of the depositional history of the Maoming oil shale. *Org Geochem* 10: 927-941.
- BRAY EE & EVANS ED. 1961. Distribution of *n*-paraffins as a clue to recognition of source beds. *Geochim Cosmochim Acta* 22: 2-15.
- BRITO AS, NOGUEIRA AC, DOS SANTOS RF, ANGÉLICA RS & RODRIGUES R. 2024. High-frequency palaeoenvironmental changes in the mixed siliciclastic-carbonate sedimentary system from a lower Permian restricted basin (West Gondwana, southern Brazil). *Sedimentology*: 1-43.
- BRITO AS, NOGUEIRA ACR, ALMEIDA LTG & DE LIMA SG. 2023. Orbital-scale cyclicity and organic matter production in a Permian shallow mixed carbonate-siliciclastic system: Paraná Basin, Brazil. *Mar Pet Geol* 147: 105987.
- BROCKS JJE & SUMMONS RE. 2014. 10.3 - Sedimentary Hydrocarbons, Biomarkers for Early Life A2 - Holland, Heinrich D. *Treatise on Geochemistry (Second Edition)*. K. K. Turekian. Oxford, Elsevier: 61-103.
- CIOCCARI GM & MIZUSAKI AMP. 2019. Sistemas petrolíferos atípicos nas Bacias Paleozoicas brasileiras – uma revisão. *Geosci Geocien* 38(2): 367-390.
- CLARK JP & PHILP R. 1989. Geochemical characterization of evaporite and carbonate depositional environments and correlation of associated crude oils in the Black Creek Basin, Alberta. *Can Pet Geol Bull* 37: 401-416.
- CONNAN J, BOUROLLEC J, DESSERT D & ALBRECHT P. 1986. The microbial input in carbonate-anhydrite facies of a

sabkha palaeoenvironment from Guatemala: a molecular approach. *Org Geochem* 10: 29-50.

CORREA DA SILVA ZC & CORNFORD C. 1985. The kerogen type, depositional environment and maturity, of the Irati Shale, Upper Permian of Paraná Basin, Southern Brazil. *Org Geochem* 8: 399-411.

DIDYK BM, SIMONEIT BRT, BRASSELL SC & EGLINTON G. 1978. Organic geochemical indicators of palaeoenvironmental conditions of sedimentation. *Nature* 272: 216-222.

ENSMINGER A, ALBRECHT P, OURISSON G & TISSOT B. 1977. Evolution of polycyclic alkanes under the effect of burial (Early Toarcian shales, Paris Basin). In: *Advances in Organic Geochemistry 1975* (Campos R and Goni J Eds), ENADIMSA, Madrid, p. 45-52.

FABIAŃSKA MJ, ĆMIEL SR & MISZ-KENNAN M. 2013. Biomarkers and aromatic hydrocarbons in bituminous coals of Upper Silesian Coal Basin: Example from 405 coal seam of the Zaleskie Beds (Poland). *Int J Coal Geol* 107: 96-111.

FOWLER MG, ABOLINS P & DOUGLAS AG. 1986. Monocyclic alkanes in Ordovician organic matter. *Org Geochem* 10: 815-823.

FRANCO N, KALKREUTH W & PERALBA MCR. 2010. Geochemical characterization of solid residues, bitumen and expelled oil based on steam pyrolysis experiments from Irati oil shale, Brazil: A preliminary study. *Fuel* 89: 1863-1871.

GELIN F, DE LEEUW JW, SINNINGHE-DAMSTÉ JS, DERENNE S & METZGER P. 1994. The similarity of chemical structures of soluble aliphatic polyaldehyde and insoluble algaenan in the green microalga *Botryococcus braunii* race A as revealed by analytical pyrolysis. *Org Geochem* 21: 423-435.

GOLDBERG K & HUMAYUN M. 2016. Geochemical paleoredox indicators in organic-rich shales of the Irati Formation, Permian of the Paraná Basin, southern Brazil. *Braz J Geol* 46(3): 377-393. DOI: 10.1590/ 2317- 4889201620160001.

GRANDE SMB, AQUINO NETO FR & MELLO MR. 1993. Extended tricyclic terpanes in sediments and petroleum. *Org Geochem* 20: 1039-1047.

GUERRA-SOMMER M & CAZZULO-KLEPZIG M. 2001. As floras gondwânicas do Paleozóico Superior do Rio Grande do Sul. *Paleontologia do Rio Grande do Sul*, Editora da UFRGS, 67-84.

HECKMANN JR, LANDAU L, GONÇALVES FTT, PEREIRA R & AZEVEDO DA. 2011. Avaliação geoquímica de óleos brasileiros com ênfase nos hidrocarbonetos aromáticos. *Quim Nova* 34(8): 1328-1333.

HOLANDA W, BERGAMASCHI S, SANTOS AC, RODRIGUES R & BERTOLINO LC. 2018. Characterization of the Assistência

Member, Irati Formation, Paraná Basin, Brazil: Organic Matter and Mineralogy. *J Sediment Environ* 3(1): 36-45.

HOLANDA W, DOS SANTOS AC, BERTOLINO LC, BERGAMASCHI S, RODRIGUES R, DA COSTA DF & JONES CM. 2019. Paleoenvironmental, paleoclimatic and stratigraphic implications of the mineralogical content of the Irati Formation, Paraná Basin, Brazil. *J South Am Earth Sci* 94: 102243.

HOLZ M, FRANÇA AB, SOUZA PA, IANNUZZI R & ROHN R. 2010. A stratigraphic chart of the Late Carboniferous/Permian succession of the eastern border of the Paraná Basin, Brazil, South America. *J South Am Earth Sci* 29: 381-399.

HONG Z-H, LI H-X, RULLKÖTTER J & MACKENZIE AS. 1986. Geochemical application of sterane and triterpane biological marker compounds in the Linyi Basin. *Org Geochem* 10: 433-439.

HUANG W-Y & MEINSCHEN WG. 1979. Sterols as ecological indicators. *Geochim Cosmochim Acta* 43: 739-745.

HUGHES WB, HOLBA AG & DZOU LIP. 1995. The ratios of dibenzothiophene to phenanthrene and pristane to phytane as indicators of depositional environment and lithology of petroleum source rocks. *Geochim Cosmochim Acta* 59(17): 3581-3598.

JIANG Z & FOWLER MG. 1986. Carotenoid-derived alkanes in oils from northwestern China. *Org Geochem* 10: 831-839.

KATES M. 1993. Membrane lipids of Archaea. In: Kates M, Kushner DJ and Matheson AT (Eds) *The Biochemistry of Archaea* (Archaeobacteria), p. 261-295. Amsterdam: Elsevier.

KELLY AE, LOVE GD, ZUMBERGE JE & SUMMONS RE. 2011. Hydrocarbon biomarkers of Neoproterozoic to Lower Cambrian oils from eastern Siberia. *Org Geochem* 42: 640-654.

KOGA Y, NISHIHARA M, MORII H & AKAGAWA-MATSUSHITA M. 1993. Ether polar lipids of methanogenic bacteria: Structures, comparative aspects, and biosynthesis. *Microbiol Rev* 57: 164-182.

LAVINA EL & LOPES RC. 1986. A transgressão marinha do Permiano Inferior e a evolução paleogeográfica do Supergrupo Tubarão no Estado do Rio Grande do Sul. *Paula Coutiana, Porto Alegre* (1): 51-103.

MACKENZIE AS & MAXWELL JR. 1981. Assessment of thermal maturation in sedimentary rocks by molecular measurements. In: *Organic Maturation Studies and Fossil Fuel Exploration* (Brooks J Ed), Academic Press, London, p. 239-254.

- MACKENZIE AS & MCKENZIE D. 1983. Isomerization and aromatization of hydrocarbons in sedimentary basins formed by extension. *Geol Mag* 120: 417-470.
- MARASCHIN AJ & RAMOS AS. 2015. Breve Abordagem Histórica sobre o Potencial Energético dos Folhelhos da Formação Irati (Bacia do Paraná) no Estado do Rio Grande do Sul. *Bol Geogr Rio Gd Sul* 25: 174-183.
- MAROTTA E, AQUINO NETO FR & AZEVEDO DA. 2014. Separação e Determinação Quantitativa dos Alcanos Lineares e dos Cíclicos/Ramificados em Petróleos Brasileiros por Aduto de Ureia e Cromatografia Gasosa: Um Estudo de Caso Revisitado. *Quim Nova* 37(10): 1692-1698.
- MARTINS CMS, CERQUEIRA JR, RIBEIRO HJPS, GARCIA KS, DA SILVA NN & QUEIROZ AFS. 2020a. Evaluation of thermal effects of intrusive rocks on the kerogen present in the black shales of Irati Formation (Permian), Paraná Basin, Brazil. *J South Am Earth Sci* 100: 102559.
- MARTINS LL, SCHULZ HM, RIBEIRO HJPS, DO NASCIMENTO CA, SOUZA ES & DA CRUZ GF. 2020b. Cadalenes and norcadalenes in organic-rich shales of the Permian Irati Formation (Paraná Basin, Brazil): Tracers for terrestrial input or also indicators of temperature-controlled organic-inorganic interactions? *J South Am Earth Sci* 100: 102559.
- MARTINS LL, SCHULZ H-M, RIBEIRO HJPS, NASCIMENTO CA, SOUZA ES & CRUZ GF. 2020c. Organic geochemical signals of freshwater dynamics controlling salinity stratification in organic-rich shales in the Lower Permian Irati Formation (Paraná Basin, Brazil). *Org Geochem* 140: 10395.
- MARZI R, TORKELOSON BE & OLSON RK. 1993. A revised carbon preference index. *Org Geochem* 20: 1303-1306. [https://doi.org/10.1016/0146-6380\(93\)90016-5](https://doi.org/10.1016/0146-6380(93)90016-5).
- MASHHADI ZS & RABBANI AR. 2015. Organic geochemistry of crude oils and Cretaceous source rocks in the Iranian sector of the Persian Gulf: An oil-oil and oil-source rock correlation study. *Int J Coal Geol* 146: 118-144.
- MATOS SA, WARREN LV, VAREJÃO FG, ASSINE ML & SIMÕES MG. 2017. Permian endemic bivalves of the "Irati anoxic event", Paraná Basin, Brazil: Taphonomical, paleogeographical and evolutionary implications. *Palaeogeogr Palaeoclimatol Palaeoecol* 469: 18-33.
- MELLO MR, TELNAES N & MAXWELL JR. 1995. The hydrocarbon source potential in the Brazilian marginal basins: a geochemical and paleoenvironmental assessment. In: *Paleogeography, Paleoclimate, and Source Rocks* (Huc A-Y Ed), American Association of Petroleum Geologists, Tulsa, OK, p. 233-272.
- MILANI EJ, FRANÇA AB & MEDEIROS RA. 2007. Rochas geradoras e rochas-reservatório da Bacia do Paraná, faixa oriental de afloramentos, Estado do Paraná. *Bol Geocien Petrobras* 15(1): 135-162.
- MOLDOWAN JM & FAGO FJ. 1986. Structure and significance of a novel rearranged monoaromatic steroid hydrocarbon in petroleum. *Geochim Cosmochim Acta* 50: 343-351.
- MOLDOWAN JM, PETERS KE, CARLSON RMK, SCHOELL M & ABU-ALI MA. 1994. Diverse applications of petroleum biomarker maturity parameters. *Arab J Sci Eng* 19: 273-298.
- MOLDOWAN JM, SUNDARARAMAN P & SCHOELL M. 1986. Sensitivity of biomarker properties to depositional environment and/or source input in the Lower Toarcian of S. W. Germany. *Org Geochem* 10: 915-926.
- MOURA AKS, SANTOS ALS & CITÓ AMGL. 2015. Otimização de Metodologia para Fracionamento Cromatográfico da Matéria Orgânica de Óleo Cru e Extratos de Rochas. XIII Congresso de Geoquímica dos países de Língua Portuguesa, p. 1.
- NADY MME, RAMADAN FS, HAMMAD MM & LOTFY NM. 2015. Evaluation of organic matters, hydrocarbon potential and thermal maturity of source rocks based on geochemical and statistical methods: Case study of source rocks in Ras Gharib oilfield, central Gulf of Suez, Egypt. *Egypt J Pet* 24: 203-211.
- NASCIMENTO CA, SOUZA ES, MARTINS LL, RIBEIRO HJPS, SANTOS VH & RODRIGUES R. 2021. Changes in depositional paleoenvironment of black shales in the Permian Irati Formation (Paraná Basin, Brazil): Geochemical evidence and aromatic biomarkers. *Mar Pet Geol* 126: 104917.
- NG C, VEGA CS & MARANHÃO MDSAS. 2019. Mixed carbonate-siliciclastic microfacies from Permian deposits of Western Gondwana: Evidence of gradual marine to continental transition or episodes of marine transgression? *Sediment Geol* 390: 62-82.
- OSORIO LL, REIS DES & RODRIGUES R. 2018. Aromatic steroids biomarkers applied to high resolution stratigraphy: Irati Formation, southern of Paraná Basin, Brazil. *J Sediment Environ* 2(4): 174-182.
- PETERS K & CASSA MR. 1993. Applied source rock geochemistry. In: *The Petroleum System - From Source to Trap* (Magoon LB and Dow WG Eds), AAPG Bulletin, Tulsa, OK, p. 93-117.
- PETERS KE, WALTERS CC & MOLDOVAN JM. 2005. *The Biomarker Guide. Biomarkers and Isotopes in the Environment and Human History*. v. 2. Ed 2nd. Cambridge University.

RABBANI AR & KAMALI MR. 2005. Source rock evaluation and petroleum geochemistry, offshore SW Iran. *J Pet Geol* 28(4): 413-428.

REIS DES, RODRIGUES R, MOLDOWAN JM, JONES CM, BRITO M, CAVALCANTE DC & PORTELA HA. 2018. Biomarkers stratigraphy of Irati Formation (Lower Permian) in the southern portion of Paraná Basin (Brazil). *Mar Pet Geol* 95: 110-138.

RIBAS L, NETO JMR, FRANÇA AB & PORTO ALEGRE HK. 2017. The behavior of Irati oil shale before and after the pyrolysis process. *J Pet Eng* 152: 156-164.

ROCHA HV, MENDES M, PEREIRA Z, RODRIGUES C, FERNANDES P, LOPES G, SANT'ANNA LG, TASSINARI CCG & LEMOS DE SOUSA MJ. 2020. New palynostratigraphic data of the Irati (Assistência Member) and the Corumbataí formations, Paraná Basin, Brazil, and correlation with other south American basins. *J South Am Earth Sci* 102: 102631.

RUBINSTEIN I & STRAUSZ OP. 1979. Geochemistry of the thiourea adduct fraction from an Alberta petroleum. *Geochim Cosmochim Acta* 43: 1387-1392.

SANTOS RV, SOUZA PA, ALVARENGA CJS, DANTAS EL, PIMENTEL MM, OLIVEIRA CG & ARAÚJO LM. 2006. Shrimp U-Pb zircon dating and palynology of bentonitic layers from the Permian Irati Formation, Paraná Basin, Brazil. *Gondwana Res* 9(4): 456-463.

SCALAN RS & SMITH JE. 1970. An improved measure of the odd-to-even predominance in the normal alkanes of sediment extracts and petroleum. *Geochim Cosmochim Acta* 34: 611-620.

SEIFERT WK & MOLDOWAN JM. 1978. Applications of steranes, terpanes and monoaromatics to the maturation, migration and source of crude oils. *Geochim Cosmochim Acta* 42: 77-95.

SEIFERT WK & MOLDOWAN JM. 1980. The effect of thermal stress on source-rock quality as measured by hopane stereochemistry. *Phys Chem Earth* 12: 229-237.

SINNINGHE DAMSTÉ JS, KENIG F & KOOPMANS MP. 1995. Evidence for gammacerane as an indicator of water column stratification. *Geochim Cosmochim Acta* 59(9): 1895-1900.

SOUZA IVF, MENDONÇA FILHO JG & MENEZES TR. 2008. Avaliação do efeito térmico das intrusivas ígneas em um horizonte potencialmente gerador da Bacia do Paraná: Formação Irati. *Braz J Geol* 32(2): 138-148.

TAO S, WANG C, DU J, LIU L & CHEN Z. 2015. Geochemical applications of tricyclic and tetracyclic terpanes biomarkers in crude oils of NW China. *Mar Pet Geol* 67: 460-467.

TEIXEIRA CAS, BELLO RMS, ALMEIDA NS, PESTILHO A, BROCHSZTAIN S, DE QUEIROZ TB, ANDRADE LS, GREGÓRIO JÚNIOR DF & SAWAKUCHI AO. 2020. Hydrocarbon generation in the Permian Irati organic-rich shales under the influence of the early cretaceous Paraná Large Igneous Province. *Mar Pet Geol* 117: 104410.

TISSOT BP & WELTE DH. 1984. Petroleum formation and occurrence, 2nd ed. Berlin, Springer-Verlag.

XAVIER PLA, SILVA AF, SOARES MB, HORN BLD & SCHULTZ CL. 2018. Sequence stratigraphy control on fossil occurrence and concentration in the epeiric mixed carbonate-siliciclastic ramp of the Early Permian Irati. *J South Am Earth Sci* 88: 157-178.

ZUMBERGE JE. 1983. Tricyclic diterpane distributions in the correlation of Paleozoic crude oils from the Williston Basin. In: *Advances in Organic Geochemistry* 1981 (Bjørø M, et al. Eds), J Wiley & Sons, New York, p. 738-745.

SUPPLEMENTARY MATERIAL

Figures S1-S16.

Table S1.

How to cite

ALMEIDA LTG, BRITO AS, CIOCCARI GM, SOUZA AA, MIZUSAKI AMP & LIMA SG. 2024. Lipid biomarker profile of the Permian organic-rich shales (Irati Formation) in the northernmost of Parana Basin, Brazil. *An Acad Bras Cienc* 96: e20230970. DOI 10.1590/0001-3765202420230970.

Manuscript received on September 2, 2023; accepted for publication on April 9, 2024

LORENA TUANE G. DE ALMEIDA¹

<https://orcid.org/0000-0003-4817-6446>

AILTON S. BRITO¹

<https://orcid.org/0000-0001-9224-5563>

GIOVANI M. CIOCCARI²

<https://orcid.org/0000-0001-9971-9709>

ALEXANDRE A. DE SOUZA¹

<https://orcid.org/0000-0002-7896-6521>

ANA MARIA P. MIZUSAKI³

<https://orcid.org/0000-0002-8205-1113>

SIDNEY G. DE LIMA¹

<https://orcid.org/0000-0001-8754-1499>

¹Programa de Pós-Graduação em Química,
Universidade Federal do Piauí/UFPI, Centro de
Ciências da Natureza, Campus Ministro Petrônio
Portella, s/n, Ininga, 64049-550 Teresina, PI, Brazil

²Universidade Federal de Pelotas, Centro de
Engenharias/CENG, Praça Domingos Rodrigues,
02, Centro, 96010-440 Pelotas, RS, Brazil

³Universidade Federal do Rio Grande do Sul, Instituto
de Geociências, Departamento de Paleontologia e
Estratigrafia, Campus do Vale, Av. Bento Gonçalves, 9500,
Prédio 43127, sala 112, 91501-970 Porto Alegre, RS, Brazil

Correspondence to: **Sidney Gonçalo de Lima**

E-mail: sidney@ufpi.edu.br

Author contributions

L.T.G. Almeida: Conceptualization, Methodology, Software, Investigation, Writing – original draft, Writing – review & editing, Visualization. A.S. Brito: Conceptualization, Writing – review & editing. G.M. Cioccarri and A.M.P. Mizusaki: Conceptualization, Resources, Writing – review & editing. A.A. Souza: Conceptualization, Formal analysis, Writing – review & editing. S. G. de Lima: Conceptualization, Methodology, Writing– review & editing, Visualization, Supervision, Funding acquisition.

